Theoretical Study on the Intracluster Elimination Channels for $Mg^+(CH_3OH)$, $Ca^+(CH_3OH)$, $Mg^+(NH_3)$, and $Ca^+(NH_3)$

Ka Wai Chan, Yang Wu, and Zhi-Feng Liu*

Department of Chemistry and Centre for Scientific Modeling and Computation Chinese, University of Hong Kong, Shatin, Hong Kong, China

Received: May 11, 2008; Revised Manuscript Received: June 24, 2008

The intracluster elimination reactions in solvated alkaline earth metal monocation clusters, M^+L_n, are known to be size-dependent, indicating links between chemical reactivity and the solvation environment controlled by the cluster size. For the methanol and ammonia clusters, there are a number of competing elimination channels involving the breaking of O−H, C−H, O−CH_3, or N−H bond. In this report, we focus on the four clusters with only one solvent molecule and systematically map out the reaction paths and intermediates. The interaction between the metal ion and the departing H atom or CH_3 group varies considerably, depending on the interaction between the metal ion and the remaining group. The understanding of the nature of these interactions and the evaluation of various theoretical levels in treating these reactions provide a solid base for the investigation of the solvation effects on the chemical reactivity of the larger clusters.

Introduction

The four ions studied in this report, $Mg^+(CH_3OH)$, $Ca^+(CH_3OH)$, $Mg^+(NH_3)$, and $Ca^+(NH_3)$, are among the simplest members of the cluster series $M^+(L)_n$, where M is an alkaline earth atom and L is a solvent molecule, such as water, methanol, or ammonia.[1−3] With an unpaired electron on M^+, these clusters provide interesting models for understanding solvation: in addition to the typical ion−solvent and solvent-solvent interactions, there is also the electron−solvent interaction, i.e., the solvation of the unpaired electron. Spectroscopically, the unpaired electron can be promoted to an unoccupied orbital, and the shift of the excitation energy as the cluster size increases has been proved to be a sensitive probe into the solvation environment, especially into the closure of the first solvation shell around the metal ion.[4−14] Such excitations also induce fragmentation in the solvent molecules, as the excitation energy is transferred into vibrational energy. However, even on the ground-state surface and at room temperature, the interplay of ion−solvent, solvent−solvent, and electron−solvent interactions can lead to very interesting changes in the solvation environment as the cluster size varies.

The best known example is $Mg^+(H_2O)_n$, for which a size-dependent H elimination channel was observed[15−17]

$$Mg^+(H_2O)_n \rightarrow (MgOH) + (H_2O)_{n-1} + H \qquad (1)$$

Remarkably, it is observed only for $5 \leq n \leq 16$, indicating a strong link between the reactivity and the microscopic solvation environment, which has been the subject of quite a few experimental and theoretical studies.[15−22] The mechanism for such size-dependent reactivity has been studied in great detail, for n starting from 1 up to 20.[18−22] It is related to the formation of an ion pair: as the number of solvent molecules increases, the unpaired electron and the Mg^{2+} are separated by solvent molecules.[20−22] With the formation of the first solvation shell around $n = 5$, the electron is screened from the Mg^{2+}, which makes it easier for a proton, produced by the acidic dissociation of a water molecule, to capture this unpaired electron for the formation of a H atom.[18,19] As n increases, the electron is further detached from the Mg^{2+} ion. When it moves into the third or forth solvation shell around the Mg^{2+}, the barrier for a proton to capture the unpaired electron becomes too high because the product OH^+ is too far away from the Mg^{2+} and can not be stabilized. This explains the switch-off of the H elimination for $n > 16$ and shows a fascinating example of the intricate links between solvation and reactivity.[19] Similar links have also been identified for the $Na(H_2O)_n$ series, which is isoelectronic with $Mg^+(H_2O)_n$.[23]

The substitutions of Mg by Ca and of H_2O by CH_3OH or NH_3 produce other series of clusters and interesting variations in the solvation environment, which have been the subject of a number of studies.[5,6,12−14,24,25] In the case of $Mg^+(CH_3OH)_n$, a hydrogen elimination channel is again observed, and interestingly it is also size dependent and active only for $5 \leq n \leq 15$, similar to that for $Mg^+(H_2O)_n$.[25] Furthermore, hydrogen elimination is also observed for $Mg^+(NH_3)_n$, after photoexcitation, while experimental evidence indicate that the reaction takes place on the vibrationally excited ground-state formed by the internal conversion of the electronically excited states.[13]

As a solvent, CH_3OH is similar to H_2O in several aspects. Dipole moments for the two solvent molecules are similar: 1.70D for CH_3OH and 1.85D for H_2O.[26] As shown in our previous study,[27] while the Mg^+−CH_3OH interaction is slightly stronger than the Mg^+−H_2O interaction, the repulsion between CH_3OH molecules are also slightly stronger than that between H_2O molecules. As a result, for both cluster series the structural trend is similar as the size increases from $n = 1$ to 6. The solvent molecules could either be crowded into the first solvation shell in direct contact with the metal ion or be positioned in the second solvation shell for more favorable solvent−solvent interactions. The energy differences among these structures are small. In addition, the shape of the SOMO is also similar for the two series $Mg^+(H_2O)_n$ and $Mg^+(CH_3OH)_n$, with the unpaired electron relatively localized, in contrast to the delocalized distribution observed in the corresponding $Mg^+(NH_3)_n$ clusters.

* To whom correspondence should be addressed. E-mail: zfliu@cuhk.edu.hk.

10.1021/jp804155t CCC: $40.75
Published on Web 08/27/2008

However, the presence of a methyl group in CH_3OH does introduce interesting complexities.[13,24,25] The reactivity of $Mg^+(CH_3OH)_n$ is therefore more complicated, since there are more elimination channels: H-eliminations, either through O−H bond or through C−H bond, and CH_3-elimination. Furthermore, the bonding nature of the other product in these elimination reactions is expected to vary considerably, among $(MOH)^+$, $(MOCH_3)^+$, $(MOHCH_2)^+$, and also $(MNH_2)^+$ for the hydrogen elimination in $M^+(NH_3)_n$.

Previous theoretical studies have reported the energetic changes for some of these elimination channels, notably the H elimination through the O−H bond for $Mg^+(CH_3OH)_n$[25] and the hydrogen elimination for $Mg^+(NH_3)_n$.[5] However, little is known about the reaction barriers and transition states involved. More importantly, as these cluster series produce variations in the solvation environment, it is interesting to systematically investigate these effects and their links to cluster reactivities.

This paper is the second among a series of studies on these clusters. In a previous paper,[27] we have identified the trends of geometrical and electronic structures for M^+L_n, with $M^+ = Mg^+$ and Ca^+, L = H_2O, CH_3OH, and NH_3, as n increases from 1 to 6. In this report, we will focus on the elimination mechanisms for the simplest members among these series, $Mg^+(CH_3OH)$, $Ca^+(CH_3OH)$, $Mg^+(NH_3)$, and $Ca^+(NH_3)$. The reaction barriers, transition states, and intermediate structures are completely mapped out and compared with the results reported before for $Mg^+(H_2O)$.[18] These results also lay the foundation for understanding the mechanisms in larger clusters, for which the solvation effects become more important as the number of solvents increases.

Computational Details

It is well understood that the nature of the bonding between the metal ion and the solvent molecule studied in this report is electrostatic.[28−30] Geometrical and electronic structures can be adequately treated by methods such as MP2 and DFT, which have been common in previous theoretical studies.[18−22] In a previous report, we have systematically varied and compared the methods and basis set sizes for the calculation of structures and solvation energy of these clusters, with $n = 1-6$.[27] For the Mg^+ clusters, there is fairly good agreement between MP2 and B3LYP results. For the Ca^+ clusters, the results are more sensitive to the choice of basis set than to the choice of method (MP2 versus B3LYP).

The problems studied in this report involve the breaking and formation of chemical bonds and are more demanding. Since these ions are relatively small in size, it is actually possible to treat them at fairly high level. It can be expected that to study reactions in larger clusters with n beyond 6, only DFT and MP2 methods could be employed due to the fast increasing computational cost. For that reason, it is also very helpful to systematically compared the DFT and MP2 results on reaction barriers with higher level methods.

Therefore, the optimization of intermediate and transition structures are attempted with a number of methods, including B3LYP, MP2, MP4, QCISD, and CCSD, with varying basis sets. Furthermore, single-point energies are also calculated at QCISD(T) and CCSD(T) levels. All calculations are performed with the Gaussian 03 package.[31] Vibrational frequencies are calculated to verify the nature of the stationary structures. As will be discussed later, there are significant fluctuations in the calculated results, depending on the level of theory. However, general agreements are found among results obtained from the highest levels, QCISD and CCSD, which are also in agreement with the single-point energy calculations at the QCISD(T) and CCSD(T) levels. In the following discussions, we use the values obtained at CCSD/6-311$^+$G** level by default, unless it is specified otherwise.

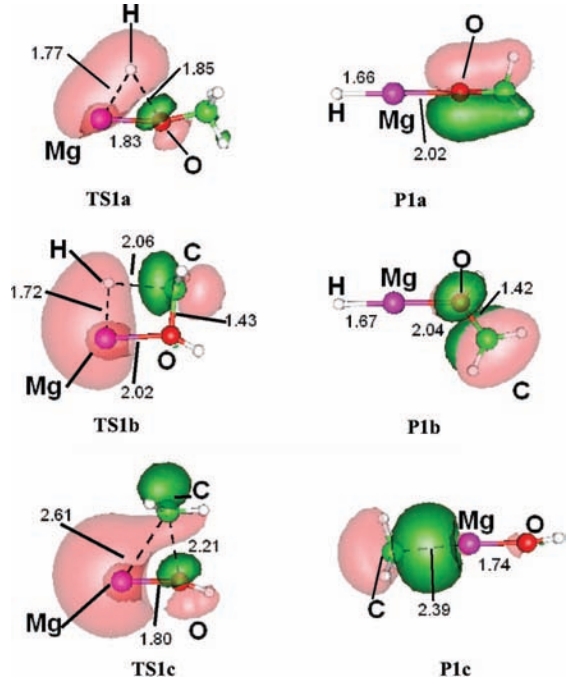

Figure 1. Products, transition structures, and SOMO plots for the elimination reactions in $Mg^+(CH_3OH)$.

Results and Discussion

1. H Elimination in $Mg^+(CH_3OH)$ through the O−H Bond. One might think that this H elimination channel in $Mg^+(CH_3OH)$ should be similar to that in $Mg^+(H_2O)_n$, since both involve the breaking of O−H bond. Experimentally the size dependence effect is indeed similar in both cluster series.[25] However, our results show that the mechanism for these two eliminations are quite distinct from each other for the case of $n = 1$. When the O−H bond is broken in $Mg^+(H_2O)$, the $(MgOH)^+$ ion could only bond to a H atom weakly, with a H−$MgOH^+$ distance at 2.26 Å. The Mg^+ ion offers little assistance for the breaking of the O−H bond in $Mg^+(H_2O)_n$.[18] However, for $Mg^+(CH_3OH)$, a metal hydride, labeled as **P1a** in Figure 1, is found as an intermediate in the hydrogen loss reaction with a significantly shorter H−Mg distance of 1.66 Å, which indicates fairly strong bonding interaction between the hydrogen atom and the Mg ion. The energy needed to break this bond is 29.3 kcal/mol calculated at the CCSD/6-311$^+$G** level and is substantially higher than the value of ∼3 kcal/mol for breaking H···$MgOH^+$. The charge on the H atom in **P1a** is more than −0.5, which indicates that it is a metal hydride bond, similar to the one reported before for $Al^+(H_2O)_n$ clusters.[32]

The barrier for the formation of **P1a** is 68.6 kcal/mol, through a transition structure **TS1a** also shown in Figure 1, while this reaction is endothermic by 50 kcal/mol. In other words, once **P1a** is formed, the barrier for it to come back to $Mg^+(CH_3OH)$ is only 18.6 kcal/mol, as compared to the barrier of 29.3 kcal/mol for H elimination by breaking the H−Mg bond.

2. H Elimination in $Mg^+(CH_3OH)$ through the C−H Bond. For $Mg^+(CH_3OH)$, the presence of a methyl group makes it possible for another H elimination channel by breaking the C−H bond. It has been argued that such a

TABLE 1: Energy Barriers and Reaction Energies (in kcal/mol) of H-Elimination from O−H Bond, C−H Bond, and CH_3-Elimination Mg^+CH_3OH at Different Levels

	H-elimination (O−H)				H-elimination (C−H)				CH_3-elimination			
	energy barrier with ZPE		reaction energy with ZPE		energy barrier with ZPE		reaction energy with ZPE		energy barrier with ZPE		reaction energy	
method												
B3LYP/6-31$^+$G**	65.7	60.1	52.6	45.0	62.8	56.7	49.7	43.5	46.8	42.6	31.7	26.3
B3LYP/6-31^{++}G**	65.6	60.0	52.5	44.7	62.9	56.7	49.6	43.5	46.8	42.6	31.7	26.3
B3LYP/6-311$^+$G**	65.7	60.1	52.6	45.0	62.5	56.0	49.0	42.8	46.5	42.1	31.7	26.2
BPW91/6-31^{++}G**	61.4	55.8	49.6	42.2	60.6	54.7	50.9	44.9	42.3	38.5	28.8	23.7
MP2/6-31$^+$G**	85.8	80.1	69.0	62.3	75.2	69.2	55.9	49.8	55.6	51.3	33.3	27.6
MP2/6-31^{++}G**	85.7	80.1	68.9	62.2	75.1	69.1	55.8	49.7	55.5	51.3	33.1	27.6
MP2/6-311$^+$G**	86.1	80.5	68.6	61.7	73.8	67.9	54.2	48.2	56.7	52.5	34.4	28.5
MP4(SDQ)/6-31^{++}G**	78.6	73.0	61.0	54.2	72.1	66.1	52.2	46.0	55.4	51.1	32.4	26.4
QCISD/6-31^{++}G**	73.7	67.9	58.4	51.4	69.2	62.6	51.3	45.0	54.3	49.7	32.3	26.2
CCSD/6-31^{++}G**	74.3	68.5	58.7	51.6	69.3	62.7	51.3	45.1	55.6	51.0	32.6	26.6
CCSD/6-311$^+$G**	74.3	68.6	57.5	50.3	67.2	60.8	49.3	43.1	56.6	52.2	33.2	27.2
					Single-Point Energy[a]							
MP4(SDTQ)/6-31^{++}G**	78.5		62.0		72.1		52.8		53.7		32.8	
QCISD(T)/6-31^{++}G**	73.0		59.1		68.6		51.8		52.8		33.1	
CCSD(T)/6-31^{++}G**	73.0		59.1		68.7		51.8		53.4		33.2	

[a] For single-point energy calculations, geometries are taken from the corresponding methods using the same basis set without triples substitutions. For example, the single-point energy at QCISD(T)/6-31^{++}G** takes the geometries from QCISD/6-31^{++}G**.

mechanism should be favored since the bond energy of C−H is lower than that for O−H by 10 kcal/mol, and statistically there are three H atoms in the methyl group, compared with only one H in the OH group.[12] In principle, the two mechanisms should be easily differentiated in a mass spectrum of $Mg^+(CH_3OD)$, although conflicting experimental evidence have been reported, probably due to the difference in the preparation of the clusters and specifically to the possible presence of excited-state Mg^+ ion during the formation of clusters.[12,25] To our best knowledge, there has been no theoretical study on such a mechanism.

We have identified a transition structure (**TS1b**) for the insertion of Mg into a C−H bond, as shown also in Figure 1, and the barrier is only 60.8 kcal/mol, compared to 68.6 kcal/mol for the insertion into the O−H bond. In addition to the lower C−H bond energy, the presence of a four atom ring (Mg−O−C−H) in the transition structure **TS1b** produces less strain as compared with the three atom ring (Mg−O−H) in **TS1a**. This reaction is also less endothermic, with an energy change of 43.1 kcal/mol, compared to the value of 50.3 kcal/mol for the O−H insertion. The insertion product, $HMg^+OH{=}CH_2$, is shown in Figure 1 as **P1b**. After the breaking of the C−H bond, the valence of the C atom is now sp^2, with a double bond between C and O atoms. The H−Mg distance at 1.67 Å is almost the same with that in **P1a**, again indicating a fairly strong bonding interaction between the H and Mg atoms. In fact, the energy required to break the H−Mg bond is 55.2 kcal/mol.

For the formation of intermediate hydride structures **P1a** and **P1b**, the barrier is lower for breaking the C−H bond than for the O−H bond. As the breaking of C−H bond is also favored statistically, it could be argued that the reaction to form **P1b** is favored on the ground-state potential surface. However, for the elimination of H atom through the breaking of the H−Mg bond, the barrier for **P1b** is considerably higher than the barrier for **P1a**, as summarized in Table 1. Considering that the formation of hydride structures is also endothermic by more than 40 kcal/mol, it is fairly unlikely that such reactions could occur on the ground state. The observation of $Mg^+(OCH_3)$ should be attributed to reactions in electronically excited states.

3. CH_3 Elimination in $Mg^+(CH_3OH)$. As observed in experiments, the CH_3 group could also be eliminated from $Mg^+(CH_3OH)_n$.[24,25] The mechanism is similar to that for H elimination, with the CH_3 group now directly bonded to the Mg ion. The SOMO (singly occupied molecular orbital) as plotted in Figure 1 (**P1c**) is obviously a C 2p orbital. It indicates very clearly that this CH_3 group is a radical, while the overall charge on the CH_3 group is close to zero (0.07). With a C−Mg distance at 2.39 Å, the SOMO almost touches the Mg ion, and in fact the energy required to completely dissociate this CH_3 group is 25.3 kcal/mol, which is only slightly lower than the value of 29.3 kcal/mol to break the H−Mg bond in **P1a**. This singly occupied C 2p orbital obviously forms a dative bond with the Mg ion.

Although the calculated barrier for CH_3 elimination is dependent on the computational method, ranging from 42.1 kcal/mol at the B3LYP/6-311$^+$G** level to ~52 kcal/mol at the MP2/6-311$^+$G** and CCSD/6-311$^+$G** levels, every method predicts that this barrier is lower than that for the hydrogen elimination, by more than 15 kcal/mol. Furthermore, with a reaction energy of 27.2 kcal/mol, it is also considerably less endothermic than hydrogen eliminations. (Table 1) Based on these two considerations, one could argue that among these three elimination channels, the CH_3 elimination is the most favorable. It is in general agreement with the collision-induced dissociation experiment, in which only CH_3-elimination is observed.[33]

4. Bonding and Charge Analysis. The intermediate structures identified for the three elimination channels in $Mg^+(CH_3OH)$ are quite distinct from each other, in terms of both the SOMO and the charge distribution.

As shown in Figure 1, the SOMO for **P1a** ($H{-}Mg^+{-}OCH_3$/O−H bond breaking) is basically an oxygen p orbital. For **P1b** ($H{-}Mg^+{-}OHCH_2$/C−H bond breaking), the SOMO is a π^* orbital, involving both the O and the C atoms. In both **P1a** and **P1b**, the SOMO stays on the oxygen side. For **P1c** ($H_3C{\cdots}Mg^+{-}OH$/O−C bond breaking), the SOMO is no longer on the O side. Instead, it is a C 2p orbital on the CH_3 radical. A doubly occupied orbital responsible for the H−Mg bond is found in both **P1a** and **P1b**.

Charge distribution, as calculated from population analysis and shown in Table 2, illustrates another interesting contrast

TABLE 2: Charge on Different Atoms of Reactant, Transition State, and Product of H-Elimination from O−H Bond, C−H Bond, and CH_3-Elimination at Different Levels[a]

H-Elimination (OH)									
	reactant			transition state			product		
method	Mg	O	H	Mg	O	H	Mg	O	H
B3LYP/6-311+G**	0.98	−0.91	0.52	1.65	−0.85	−0.18	1.50	−0.53	−0.52
MP2/6-311+G**	0.99	−0.90	0.51	1.74	−0.78	−0.33	1.53	−0.43	−0.57
CCSD/6-311+G**	0.99	−0.89	0.51	1.72	−0.85	−0.24	1.51	−0.44	−0.55
H-Elimination (OH)									
	reactant			transition state			product		
method	Mg	O	H	Mg	O	H	Mg	O	H
B3LYP/6-311+G**	0.98	−0.91	0.19	1.39	−0.89	−0.43	1.47	−0.87	−0.52
MP2/6-311+G**	0.99	−0.90	0.18	1.49	−0.89	−0.49	1.53	−0.87	−0.57
CCSD/6-311+G**	0.99	−0.89	0.18	1.41	−0.88	−0.42	1.50	−0.86	−0.55
CH_3-Elimination									
	reactant			transition state			product		
method	Mg	O	CH_3	Mg	O	CH_3	Mg	O	CH_3
B3LYP/6-311+G**	0.98	−0.91	0.40	1.52	−1.24	0.20	1.74	−1.25	0.01
MP2/6-311+G**	0.99	−0.90	0.40	1.48	−1.25	0.26	1.85	−1.43	0.07
CCSD/6-311+G**	0.99	−0.89	0.40	1.49	−1.20	0.20	1.84	−1.41	0.07

[a] All the charges are calculated by natural population analysis.

between both **P1a** and **P1b** on the one hand, and **P1c** on the other. In the former, the to-be-eliminated hydrogen is negatively charged, with a value close to −0.5, and is actually as negative as the O atom. Both the H−Mg and O−Mg bonding interactions can be roughly described as a polarized covalent bond. In the latter, while the charge on the to-be-eliminated CH_3 group is almost zero, the charge on the O atom jumps to ∼−1.3. There is also an appreciable increase in the positive charge on Mg, which is now around +1.8. The interaction between Mg and O in this case can be characterized as the ionic interaction between Mg^{2+} and OH^+.

In fact, the charge distribution on the $(MgOH)^+$ part of **P1c** is quite similar to that in $H\cdots(MgOH)^+$, the intermediate structure for the H elimination in $Mg^+(H_2O)$. In both cases, the $(MgOH)^+$ is dominated by ionic interaction between Mg^{2+} and OH^-, while the unpaired electron is shifted to the departing radical CH_3 or to the radical H in the case of $Mg^+(H_2O)$. The contrast between the two cases is in the interaction between the radical and the Mg ion. In $H\cdots(MgOH)^+$, the SOMO is a spherical H 1s orbital and its interaction with the Mg ion is fairly weak. In $CH_3\cdots(MgOH)^+$, the SOMO is a more pointed C 2p orbital and the interaction between CH_3 and Mg ion is more significant, with a dissociation energy of 25.3 kcal/mol, which is a good example of the difference in the properties between H and CH_3 group.

For the two H elimination channels in $Mg^+(CH_3OH)$, the Mg−O interaction is less ionic in the products $(Mg-O\ CH_3)^+$ and $(Mg-OHCH_2)$. It is more favorable for the H atom to stay close to the Mg ion for its stabilization. And judging from the energy required to break it, the Mg−H bond is quite strong.

5. Elimination Channels in $Ca^+(CH_3OH)$. While the Mg−O bonding in the elimination intermediate could either be ionic or covalent, depending on the reaction channel, the replacement of Mg by Ca is expected to be more favorable for the ionic interactions. The valence electron on Ca^+ is less tightly bound than that in Mg^+. Furthermore, the more diffusive valence orbitals on Ca^+ make it less favorable for covalent interactions.

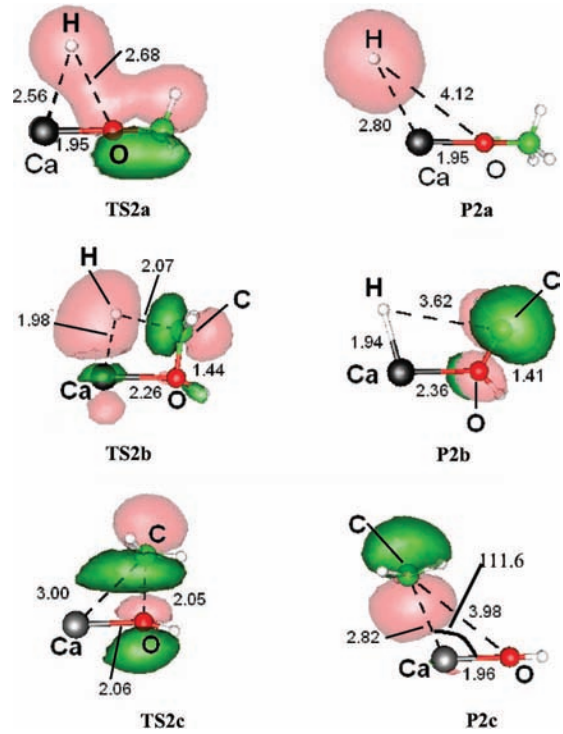

Figure 2. Products, transition structures, and SOMO plots for the elimination reactions in $Ca^+(CH_3OH)$.

The same three elimination channels for $Mg^+(CH_3OH)$ are also identified for Ca^+ (CH_3OH), as shown in Figure 2. The most significant change is observed for the H elimination through O−H breaking. The barrier at 46.6 kcal/mol is only slightly higher than the reaction energy at 46.3 kcal/mol, as shown in Table 3. The SOMO is obviously a H 1s orbital. With a H−Ca distance at 2.8 Å, the interaction between H and Ca is weak and the energy required to completely eliminate the H atom from **P2a** is only 1.4 kcal/mol. This channel is therefore in sharp contrast to that in Mg^+ (CH_3OH), but is very similar

TABLE 3: Energy Barriers and Reaction Energies (in kcal/mol) of H-Elimination from O−H Bond, C−H Bond, and CH_3-Elimination Ca^+CH_3OH at Different Levels

	H-elimination (O−H)		H-elimination (C−H)		CH_3-elimination	
method	energy barrier with ZPE	reaction energy with ZPE	energy barrier with ZPE	reaction energy with ZPE	energy barrier	reaction energy with ZPE
B3LYP/6-31$^+$G**	58.2	50.6	55.0	48.1	66.1	59.1	60.3	53.4	39.0	34.9	25.2	19.9
B3LYP/6-311$^+$G**	42.2	35.4	42.2	35.5	54.5	47.6	50.9	44.4	28.2	24.3	5.1	0.0
B3LYP/6-311$^+$G(3df,3pd)	39.0	32.2	39.0	32.3	52.5	46.0	49.2	42.8	27.2	23.5	2.47	−2.8
MP2/6-31$^+$G**	61.2	54.2	60.4	53.4	78.6	71.9	68.3	61.5	51.1	47.4	24.1	19.0
MP2/6-311$^+$G**	49.3	42.6	48.3	41.3	69.4	62.6	60.9	54.6	45.6	42.1	14.9	9.6
MP2/6-311$^+$G(3df,3pd)	41.8	35.2	41.0	34.2	64.8	58.0	57.8	51.5	39.5	36.4	8.1	2.9
QCISD/6-311$^+$G**	52.7[a]	45.7[a]	52.7	45.7	64.9	58.1	57.1	50.6	39.9	35.5	14.9	9.5
CCSD/6-311$^+$G**	53.6	46.6	53.3	46.3	65.3	58.5	57.2	50.8	43.3	39.2	15.3	9.9
Single-Point Energy[b]												
QCISD(T)/6-311$^+$G**	51.8		51.7		64.4		57.4		44.3		15.2	
QCISD(T)/6-311$^+$G(3df,3pd)	44.5		44.5		59.8		53.9		38.0		8.0	
CCSD(T)/6-311$^+$G**	52.0		52.0		64.5		57.5		40.8		15.4	
CCSD(T)/6-311$^+$G(3df,3pd)	44.7		44.8		59.9		54.0		36.2		8.2	

[a] There are two imaginary frequencies in TS of H-elimination calculated at QCISD/6-311$^+$G** method. [b] For single-point energy calculations, geometries are taken from the corresponding methods with the basis set 6-311$^+$G**without triples or quadruples substitutions. For example, the single-point energy calculations at QCISD(T)/6-311$^+$G** and QCISD(T)/6-311$^+$G(3df,3pd) take the geometries from QCISD/6-311$^+$G**.

to the H elimination in Mg^+ (H_2O), with a H radical weakly bound to $(CaO\ CH_3)^+$ in **P2a**.

Charge analysis results, as shown in Table 4, are consistent with the above observation. In **P2a**, the negative charge on the O atom around −1.2 is considerably higher than the value around −0.5 in **P1a**, while the charge on the metal atom is also higher (+1.8 in H···Ca^+OCH_3 versus +1.5 in H···Mg^+OCH_3). As mentioned earlier, ionic interaction is more favored for the Ca ion and the interaction in Ca^+OCH_3 is indeed more ionic, and is similar to that in $(MgOH)^+$. H−Ca bonding is no longer needed to stabilize Ca^+OCH_3, while the energy barrier at 46.6 kcal/mol is lower than the barrier of 68.6 kcal/mol for the same H elimination in $Mg^+(CH_3OH)$.

The other two elimination channels are similar to their corresponding $Mg^+(CH_3OH)$ channels. For the H elimination through C−H bond breaking, a stable intermediate **P2b** is identified, in which there is again bonding interaction between H and Ca. Understandably, the Ca−H distance at 1.94 Å is longer than the corresponding Mg−H distance. The energy required to break the Ca−H bond is 46.4 kcal/mol, which is 9 kcal/mol less than that for Mg−H bond, but nonetheless substantial. The charges on Ca and O for **P2b** are similar to those for **P1b**. The only notable difference is that the O−Ca−H angle is no longer 180°, which probably indicates less steric repulsion between the hydride H and the O═CH_3 group. The barrier height at 58.5 kcal/mol is comparable to the value of 60.8 kcal/mol for $Mg^+(CH_3OH)$. This barrier is also higher than that for breaking the O−H bond, reversing the ordering as observed for $Mg^+(CH_3OH)$, which should be attributed to the less favorable Ca−O covalent interaction.

For the elimination of CH_3, an intermediate structure (**P2c**) is again identified, with a radical CH_3 group bound to a $(CaOH)^+$ core. The C−Ca distance is increased to 2.8 Å, while the C−Ca−O angle is bent to 111.6°. The barrier at 39.2 kcal/mol is the lowest among all these elimination channels, which can be attributed to the more favorable ionic interaction in $(CaOH)^+$. It is also in broad agreement with the experimental observation of this channel.[25] Similar to **P1c**, there is some bonding interaction between the carbon atom and the Ca ion, through the SOMO which is basically a C 2p orbital. However, the energy required to completely dissociate the CH_3 group is now only 11 kcal/mol.

It is also interesting to notice a structural difference between the intermediate structures for $Ca^+(CH_3OH)$ and for $Mg^+(CH_3OH)$. While for $Mg^+(CH_3OH)$, the to-be-eliminated group or atom is on the opposite site of the remaining group, the corresponding intermediate structures for $Ca^+(CH_3OH)$ are bent, since it is more spacious around the Ca^+ ion. The same contrast is also observed for $Mg^+(NH_3)$ and $Ca^+(NH_3)$.

6. H Elimination in $Mg^+(NH_3)$ and $Ca^+(NH_3)$. With ammonia as the solvent, the elimination is simplified to one channel, H elimination, similar to the hydrated clusters. The N−H bond energy in NH_3 at 108.2 kcal/mol is slightly larger than the O−H bond energy (104.2 kcal/mol) in CH_3OH.[26] In terms of the mechanism, it resembles the H elimination in the methanol clusters. As shown in Figure 3a, a stable intermediate with a H-metal bond is found for both $Mg^+(NH_3)$ (**P3a**) and $Ca^+(NH_3)$ (**P3b**), in agreement with a previous ab initio study.[5] The dissociation energy for breaking the M-H bond is 40.4 kcal/mol for H−$MgNH_2^+$, but decreases substantially to 11.2 kcal/mol for H−$CaNH_2^+$. Obviously, the Mg−NH_2 interaction is less ionic than the Mg−OH interaction and more similar to the Mg−OCH_3 interaction, which makes it possible for substantial interaction

TABLE 4: Charge on Different Atoms of Reactant, Transition State, and Product of H-Elimination from O−H Bond, C−H Bond, and CH_3-Elimination at Different Levels[a]

H-Elimination (OH)

	reactant			transition state			product		
method	Ca	O	H	Ca	O	H	Ca	O	H
B3LYP/6-31$^+$G**	1.01	−0.93	0.55	1.76	−0.77	−0.39	1.80	−0.81	−0.40
B3LYP/6-311$^+$G**	0.99	−0.89	0.51	1.80	−1.14	0.02	1.80	−1.14	0.02
B3LYP/6-311$^+$G(3df,3pd)	0.98	−0.88	0.51	1.79	−1.13	0.02	1.79	−1.13	0.02
MP2/6-311$^+$G**	1.00	−0.88	0.50	1.85	−1.11	−0.05	1.86	−1.17	0.01
MP2/6-311$^+$G(3df,3pd)	1.00	−0.88	0.51	1.85	−1.12	−0.05	1.84	−1.17	0.01
CCSD/6-311$^+$G**	1.00	−0.87	0.49	1.87	−1.17	−0.01	1.87	−1.19	0.01

H-Elimination (CH)

	reactant			transition state			product		
method	Ca	C	H	Ca	C	H	Ca	C	H
B3LYP/6-31$^+$G**	1.01	−0.35	0.23	1.54	−0.12	−0.49	1.54	−0.09	−0.56
B3LYP/6-311$^+$G**	0.99	−0.21	0.19	1.66	−0.11	−0.54	1.62	−0.01	−0.65
B3LYP/6-311$^+$G(3df,3pd)	0.98	−0.20	0.19	1.67	−0.16	−0.54	1.63	−0.02	−0.66
MP2/6-311$^+$G**	1.00	−0.18	0.18	1.69	−0.12	−0.53	1.69	0.02	−0.71
MP2/6-311$^+$G(3df,3pd)	1.00	−0.19	0.18	1.74	−0.14	−0.57	1.71	0.00	−0.73
CCSD/6-311$^+$G**	1.00	−0.16	0.17	1.65	−0.07	−0.52	1.67	0.03	−0.69

CH_3-Elimination

	reactant			transition state			product		
method	Ca	O	CH_3	Ca	O	CH_3	Ca	O	CH_3
B3LYP/6-31$^+$G**	1.01	−0.93	0.38	1.59	−1.24	0.11	1.93	−1.48	0.03
B3LYP/6-311$^+$G**	0.99	−0.89	0.39	1.43	−1.16	0.21	1.82	−1.36	0.03
B3LYP/6-311$^+$G(3df,3pd)	0.99	−0.89	0.39	1.41	−1.14	0.21	1.82	−1.35	0.03
MP2/6-311$^+$G**	1.00	−0.88	0.38	1.51	−1.15	0.13	1.87	−1.39	0.02
MP2/6-311$^+$G(3df,3pd)	1.00	−0.88	0.38	1.50	−1.13	0.11	1.86	−1.38	0.02
CCSD/6-311$^+$G**	1.00	−0.87	0.38	1.51	−1.14	0.14	1.88	−1.39	0.02

[a] All the charges are calculated by natural population analysis.

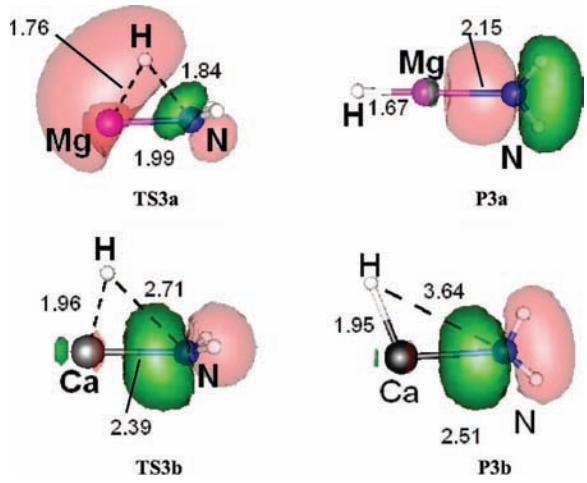

Figure 3. Products, transition structures, and SOMO plots for the hydrogen elimination reaction in $Mg^+(NH_3)$ and $Ca_3(NH_3)$.

between the hydrogen and the Mg ion. In $Ca^+(NH_3)$, the Ca atom is more positively charged and the Ca−NH_2 interaction is more ionic, which significantly weakens the H−Ca binding energy. The DFT results disagree with the post Hartree−Fock results regarding the charges on the N and the hydride H atom. The reaction barriers are comparable to those found for the methanol solvated clusters.

7. Comparison of Methods. Considerable fluctuations are found for both the calculated reaction barriers and energies. Disagreement between the MP2 and DFT reaches 20 kcal/mol, depending on the basis set. A general pattern emerges from the results listed in Tables 1−6: the MP2 value is always higher than the corresponding DFT value, for both the reaction barrier and energy.

For $Mg^+(L)$, the CI and coupled-cluster (CC) results are in good agreement with each other. Single-point calculations with more configurations produce only very small shifts,

TABLE 5: Energy Barriers and Reaction Energies (in kcal/mol) of H-Elimination from N−H Bond at Different Levels

method	energy barrier with ZPE		reaction energy with ZPE	
B3LYP/6-31$^+$G**	72.3	66.2	58.2	51.7
B3LYP/6-31^{++}G**	72.2	66.1	58.1	51.6
B3LYP/6-311$^+$G**	71.7	65.7	57.6	51.2
BPW91/6-31^{++}G**	69.8	63.7	60.3	54.0
MP2/6-31$^+$G**	88.2	82.9	64.9	58.6
MP2/6-31^{++}G**	88.0	82.7	64.8	58.5
MP2/6-311$^+$G**	86.9	81.8	63.7	57.5
MP4(SDQ)/6-31^{++}G**	82.9	77.8	58.3	51.8
QCISD/6-31^{++}G**	78.8	72.9	57.5	51.0
CCSD/6-31^{++}G**	79.1	73.0	57.4	50.9
CCSD/6-311$^+$G**	77.3	71.4	55.7	49.3
Single-Point Energy[a]				
MP4(SDTQ)/6-31^{++}G**	82.6		59.3	
QCISD(T)/6-31^{++}G**	77.9		58.3	
CCSD(T)/6-31^{++}G**	78.0		58.3	

[a] For single-point energy calculations, geometries are taken from the corresponding methods using the same basis set without triples substitutions. For example, the single-point energy at QCISD(T)/6-31^{++}G** takes the geometries from QCISD/6-31^{++}G**.

TABLE 6: Energy Barriers and Reaction Energies (In kcal/mol) of H-Elimination from N−H Bond in Ca^+NH_3 at Different Levels

method	energy barrier with ZPE		reaction energy with ZPE	
B3LYP/6-31$^+$G**	67.9	60.6	66.6	59.6
B3LYP/6-311$^+$G**	59.9	52.7	58.5	51.6
B3LYP/6-311$^+$G(3df,3pd)	58.9	51.7	57.1	50.2
MP2(full)/6-31$^+$G**	82.2	75.5	76.7	69.5
MP2(full)/6-311$^+$G**	73.6	67.0	70.8	64.1
MP2(full)/6-311$^+$G(3df,3pd)	71.2	64.5	69.4	62.8
QCISD/6-311$^+$G**	65.3	58.3	64.0	57.1
CCSD/6-311$^+$G**	65.7	58.7	64.0	57.1
Single-Point Energy[a]				
QCISD(T)-SP/6-311$^+$G**	66.0		64.9	
QCISD(T)-SP/6-311$^+$G(3df,3pd)	63.3		62.8	
CCSD(T)-SP/6-311$^+$G**	66.0		64.8	
CCSD(T)-SP/6-311$^+$G(3df,3pd)	63.1		62.8	

[a] For single-point energy calculations, geometries are taken from the corresponding methods with the basis set 6-311$^+$G** without triples substitutions.

within 2 kcal/mol. These results can be regarded as the benchmark for comparison with the MP2 and DFT results. Again, there is a fairly general pattern: the CI and CC values are usually between the corresponding MP2 and DFT values. In other words, while MP2 methods overestimate the barrier and reaction energy, DFT methods underestimate them. The magnitude of error is comparable. As far as accuracy is concerned, there is no obvious advantage for choosing MP2 over DFT, or vice versa.

Similar patterns are also observed for $Ca^+(L)$. However, there is one significant difference: the calculated values for $Ca^+(CH_3OH)$ is very sensitive to the basis set employed and varies by as much as 15 kcal/mol for the same method. This is true for both MP2 and DFT methods, and also true for CI and CC methods, albeit with smaller fluctuations. In DFT calculations, the smallest basis set 6-31$^+$G** usually produces the highest energetic values. Since these values are generally underestimated by DFT methods, the B3LYP/6-31$^+$G** turns out to be the best in reproducing the CI and CC energetic value. A similar observation was made before in previous studies on $Mg^+(H_2O)_n$ and $Na^+(H_2O)_n$.[19,23] It indicates that B3LYP/6-31$^+$G** is an excellent compromise between computational cost and accuracy, at least for the solvated magnesium clusters. Unfortunately, it is more problematic for the solvated calcium clusters, specifically in the case of H elimination through O−H bond for $Ca^+(CH_3OH)$, for which the charge distribution obtained by B3LYP/6-31$^+$G** is in serious disagreement with results obtained by other methods.

Despite the differences among the values obtained by various methods, there are general agreements about the nature of the intermediate structures, the geometrical parameters, and more importantly the ordering of barrier height and reaction energy among various channels for a specific cluster.

Summary

The H and CH_3 elimination channels for M^+L, with M = Mg^+ and Ca^+, and L = CH_3OH and NH_3, have been systematically examined by ab initio and DFT methods. Considerable variations are found for the transition and intermediate structures.

For the CH_3 elimination, the breaking of C−O bond produces a methyl radical which interacts with the metal ion through a dative bond. Its reaction barrier is lower than the corresponding H elimination channel.

In the case of $M^+(CH_3OH)$, transition and intermediate structures have been identified for hydrogen elimination through either the O−H and the C−H bond. The breaking of either the O−H bond or a C−H bond leads to a hydride structure in which the bonding interaction between H and the metal is quite strong. The same applies to the hydrogen elimination for $M^+(NH_3)$. The only exception is the H elimination for $Ca^+(CH_3OH)$ through the breaking of O−H bond, which produces a H atom weakly bound to the cluster and is the only case similar to the H elimination in $Mg^+(H_2O)$. The important factor is the metal-solvent interaction after the bond breaking step. When it is charge polarized and ionic, the eliminated H would become a H atom. When it has a considerable covalent character and is less polarized, the H would bond with the metal ion to stabilize the product.

The interaction energy between the departing H or CH_3 group and the metal ion varies considerably depending on the metal, the solvent and the elimination channel, from a few kcal/mol to more than 50 kcal/mol. How would these reactions change when more solvent molecules are added to the cluster should be interesting problems, for probing the link between reactivity and solvation, which will be taken up in a followup study.

TABLE 7: Charge on Different Atoms of Ground State, Transition State, and Product of H-Elimination from N−H Bond in MNH_3 where M = Mg^+ and Ca^+ at Different Levels[a]

Mg^+NH_3	ground state			transition state			product		
method	Mg	N	H	Mg	N	H	Mg	N	H
B3LYP/6-311$^+$G**	0.95	−1.19	0.41	1.57	−1.09	−0.25	1.44	−0.67	−0.52
MP2/6-311$^+$G**	0.96	−1.19	0.41	1.85	−1.29	−0.35	1.50	−0.66	−0.57
CCSD/6-311$^+$G**	0.96	−1.16	0.40	1.60	−1.05	−0.29	1.48	−0.64	−0.55
Ca^+NH_3	ground state			transition state			product		
method	Ca	N	H	Ca	N	H	Ca	N	H
B3LYP/6-31$^+$G**	0.99	−1.31	0.44	1.63	−0.93	−0.50	1.69	−1.02	−0.48
B3LYP/6-311$^+$G**	0.97	−1.19	0.40	1.65	−0.77	−0.59	1.73	−0.99	−0.47
B3LYP/6-311$^+$G(3df,3pd)	0.97	−1.18	0.41	1.65	−0.77	−0.60	1.74	−1.02	−0.45
MP2/6-311$^+$G**	0.99	−1.17	0.40	1.73	−0.77	−0.66	1.67	−0.65	−0.71
MP2/6-311$^+$G(3df,3pd)	0.98	−1.18	0.40	1.73	−0.74	−0.70	1.69	−0.67	−0.73
CCSD/6-311$^+$G**	0.98	−1.14	0.39	1.70	−0.73	−0.65	1.65	−0.64	−0.69

[a] All of the charges are calculated by natural population analysis.

Acknowledgment. Calculations reported in this paper were performed on the computer clusters operated by the Department of Chemistry, the Chinese University of Hong Kong (CUHK), supported by a Special Equipment Grant, and on the SGI Origin 2000, at the Information Technology Services Center (ITSC), CUHK. We thank Mr. Ka Fai Woo at the Department of Chemistry and Mr. Frank Ng at ITSC, for technical supports. We gratefully acknowledge the financial support provided by the Hong Kong SAR Government, through the Project CUHK 401604P.

References and Notes

(1) Farrar, J. M. *Int. Rev. Phys. Chem.* **2003**, *22*, 593.
(2) Castleman, A. W., Jr.; Bowen, K. H. *J. Phys. Chem.* **1996**, *100*, 12911.
(3) Fuke, K.; Hashimoto, K.; Iwat, S. *Chem. Phys.* **1999**, *110*, 431.
(4) Misaizu, F.; Sanekata, M.; Fuke, K.; Iwata, S. *J. Chem. Phys.* **1994**, *100*, 1161.
(5) Yoshida, S.; Daigoku, K.; Okai, N.; Takahata, A.; Sabu, A.; Hashimoto, K.; Fuke, K. *J. Chem. Phys.* **2002**, *117*, 8657.
(6) Yoshida, N.; Okai, K.; Fuke, K. *Chem. Phys. Lett.* **2001**, *347*, 93.
(7) Misaizu, F.; Sanekata, M.; Tsukamoto, K.; Fuke, K.; Iwata, S. *J. Phys. Chem.* **1992**, *96*, 8259.
(8) Shen, M. H.; Winniczek, J. W.; Farrar, J. M. *J. Phys. Chem.* **1987**, *91*, 6447.
(9) Shen, M. H.; Winniczek, J. W.; Farrar, J. M. *J. Phys. Chem.* **1987**, *91*, 6447.
(10) Donnelly, S. G.; Farrar, J. M. *J. Chem. Phys.* **1993**, *98*, 5450.
(11) Shen, M. H.; Farrar, J. M. *J. Chem. Phys.* **1991**, *94*, 3322.
(12) Lee, J. I.; Sperry, D. C.; Farrar, J. M. *J. Chem. Phys.* **2001**, *114*, 6180.
(13) Lee, J. I.; Sperry, D. C.; Farrar, J. M. *J. Chem. Phys.* **2004**, *121*, 8375.
(14) Willey, K. F.; Yeh, C. S.; Robbins, D. L.; Pilgrim, J. S.; Duncan, M. A. *J. Chem. Phys.* **1992**, *97*, 8886.
(15) Harms, A. C.; Khanna, S. N.; Chen, A. B.; Castleman, A. W. *J. Chem. Phys.* **1994**, *100*, 3540.
(16) Sanekata, M.; Misaizu, F.; Fuke, K.; Iwata, S.; Hashimoto, K. *J. Am. Chem. Soc.* **1995**, *117*, 747.
(17) Berg, C.; Beyer, M.; Achatz, U.; Joos, S.; Niedner-Schatteburg, G.; Bondybey, V. E. *Chem. Phys* **1998**, *239*, 379.
(18) C, K.; Siu, Z. F.; Liu, *Chem EuJ.* **2002**, *8*, 3177.
(19) Siu, C. K.; Liu, Z. F. *Phys. Chem. Chem. Phys.* **2005**, *7*, 1005.
(20) Watanabe, H.; Iwata, S.; Hashimoto, K.; Misaizu, F.; Fuke, K. *J. Am. Chem. Soc.* **1995**, *117*, 755.
(21) Reinhard, B. M.; Niedner-Schatteburg, G. *J. Chem. Phys.* **2003**, *118*, 3571.
(22) Reinhard, B. M.; Niedner-Schatteburg, G. *Phys. Chem. Chem. Phys.* **2002**, *4*, 1471.
(23) Chan, K. W.; Siu, C. K.; Wong, S. Y.; Liu, Z. F. *J. Chem. Phys.* **2005**, *123*, 124313.
(24) Woodward, C. A.; Dobson, M. P.; Stace, A. J. *J. Phys. Chem. A* **1997**, *101*, 2279.
(25) Lu, W. Y.; Yang, S. H. *J. Phys. Chem. A* **1998**, *102*, 825.
(26) Lide, D. R., Ed.; *CRC Handbook of Chemistry and Physics*, 77th ed.; CRC Press: Boca Raton, FL, 1997.
(27) Chan, K. W.; Wu, Y.; Liu, Z. *Can. J. Chem.* **2007**, *85*, 873.
(28) Sodupe, M.; Bauschlicher, C W. *Chem. Phys. Lett.* **1992**, *195*, 494.
(29) Bauschlicher, C. W.; Sodupe, M.; Partridge, H. *J. Chem. Phys.* **1992**, *96*, 4453.
(30) Bauschlicher, C. W.; Partridge, H. *J. Phys. Chem.* **1991**, *95*, 9694.
(31) Frisch, M. J.; Trucks, G. W.; Schlegel, H. B.; Scuseria, G. E.; Robb, M. A.; Cheeseman, J. R.; Zakrzewski, V. G.; Montogemery, J. A.; Stratmann, R. E.; Burant, J. C.; Dapprich, S.; Millam, J. M.; Daniels, A. D.; Kudin, K. N. Strain, M. C.; Farkas, O.; Tomasi, J.; Barone, V.; Cossi, M.; Cammi, R.; Mennucci, B.; Pomelli, C. Adamo, C.; Clifford, S.; Ochterski, J.; Petersson, G. A.; Ayala, P. Y.; Cui, Q.; Morokuma, K.; Malick, D. K.; Rabuck, A. D.; Raghavachari, K.; Foresman, J. B.; Cioslowski, J.; Ortiz, J. V. Stefanov, B. B.; Liu, G.; Liashenko, A.; Piskorz, P.; Komaromi, I.; Gomperts, R.; Martin, R. L.; Fox, D. J.; Keith, T.; Al-Laham, M. A.; Peng, C. Y.; Nanayakkara, A.; Gonzelez, C. Challacombe, M.; Gill, P. M. W.; JohnsonB.; Chen, W.; Wong, M. W.; Andres, J. L.; Gonzalez, C.; Head-Gordon, M.; Replogle, E. S.; Pople, J. A. Gaussian 98, revision A.11; Gaussian, Inc.: Pittsburgh, PA, 1998.
(32) Siu, C. K.; Liu, Z. F.; Tse, J. S. *J. Am. Chem. Soc.* **2002**, *124*, 10846.
(33) Andersen, A.; Muntean, F.; Walter, D.; Rue, C.; Armentrout, P. B. *J. Phys. Chem. A* **2000**, *104*, 692.

JP804155T